PHARMACOLOGIC INHIBITION OF INTEGRIN α4β7 BY SMALL MOLECULE INHIBITOR ARRESTS B LYMPHOCYTE TRAFFICKING TO MURINE GUT-ASSOCIATED LYMPHOID TISSUES

Naresh S. Redhu[1], Allison Sang[1], Dooyoung Lee[1], Fyonn Dhang[1], Michael Rowe[1], Vinod Yadav[1], Ali Hussain[1], Bryce Harrison[1], Maloy Mangada[1], Sarah St. Gelais[1], Dawn Troast[1], Cheng Zhong[1], Xiaomei Ge[2], Lili Sun[2], Wei Wang[2], Dan Cui[1], Matthew Bursavich[1], Blaise Lippa[1], Bruce N. Rogers[1], Adrian S. Ray[1], and Jamie Wong[1]

[1]Morphic Therapeutic, 35 Gatehouse Drive, Waltham, Massachusetts, USA, 02451 ; [2]Biology & Pharmacology Department, Shanghai ChemPartner Co. Ltd., Pudong, Shanghai, 201203, P.R. China.

INTRODUCTION

The integrin α4β7 through its interaction with mucosal addressin cell adhesion molecule 1 (MAdCAM-1) impacts the homing of lymphocytes to gut-associated lymphoid tissues (GALT), including Peyer's patches (PP). Clinical data from IBD patients treated with α4β7 inhibiting antibody vedolizumab have shown reduced B cell trafficking to the intestinal compartment. Both the colonic lymphoid aggregates and PP serve as immune inductive secondary lymphoid structures responsible for mucosal immunoglobulin response generation and the pathophysiology of IBD. The current study was aimed at mechanistically defining the effects of MT-101, a potent and selective small molecule α4β7 integrin inhibitor, on cellular dynamics in the GALT and colonic lamina propria (LP) of naïve mice.

METHODS

Mn-free Mouse Whole Blood Receptor Occupancy Assay

Flow cytometry-based receptor occupancy (RO) assays for α4β7 was established under physiologic conditions including natural ligand mucosal vascular addressin cell adhesion molecule-1 (MAdCAM-1), in the absence of manganese (Redhu et al., AAI 2021; Mangada et al., 2020). Briefly, MT-101 was assessed for its 50% and 90% inhibition constants (IC_{50} and IC_{90}) for α4β7 on $CD4^+CD44^{hi}$ memory T cells in fresh mouse blood pooled from 20-40 animals per experiment. The blood was treated *ex vivo* with varying concentrations of MT-101 and stained with fluorescently labeled antibodies forCD44, CD3, CD4, integrin α4, integrin β7, viability, and Free and Total α4β7 probes. The cells were acquired using BD FACS CantoII and the data analyzed using FlowJo.

Peyer's Patch Decellularization Assay: To determine the effect of α4β7 inhibition on steady state immune cell trafficking to the gastrointestinal tract, an acute Peyer's Patch decellularization (PP decell) assay was developed (Mangada et al., UEG 2020). We investigated the effect of MT-101 and anti-α4β7 blocking antibody (DATK32) on PP cellularity enumerated by multicolor flow cytometry (Figure 1).

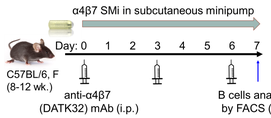

Figure 1: Mouse PP decellularization assay scheme. *Naïve C57BL/6 mice were administered small molecule α4β7 inhibitor MT-101 (30mg/ml, 0.5ul/hr, day 0-7) or anti-α4β7 blocking antibody (DATK32, 300µg/mouse, 3x per week) as shown. B cells in PP were analyzed on day 7 by flow cytometry.*

GALT and Colon LP single cell and histopathological analysis: To explore the effects on cellular dynamics in GALT and colonic lamina propria (LP) of naïve mice in an unbiased fashion, animals were treated with MT-101 via s.c. minipump or i.p. injection of DATK32 (Figure 1), and the PP and colonic tissues were collected for (i) histopathological analysis, and (ii) single-cell (sc)RNAseq analysis.

Single cell suspensions were prepared by mechanically dissociating PP, whereas the LP immune cells were prepared as we reported previously (*Redhu et al., eLife 2017*). Briefly, colons were stripped of epithelial cells by performing agitation in 10 mM EDTA for 20 min at 37ºC before digestion in collagenase VIII (Sigma-Aldrich) for 45 min at 37ºC. Undigested tissue were disrupted by repeated flushing through a 10ml syringe without the needle. Single cell suspensions were filtered and stained for flow cytometry-based cell sorting (Sony MA 900 sorter). Live $CD45^+$ cells were sorted from PP and LP cell fractions and subjected to scRNAseq library preparation using 10X Genomics' Chromium Single cell 3' reagent v3 kit. Data analysis was performed using the R studio.

RESULTS

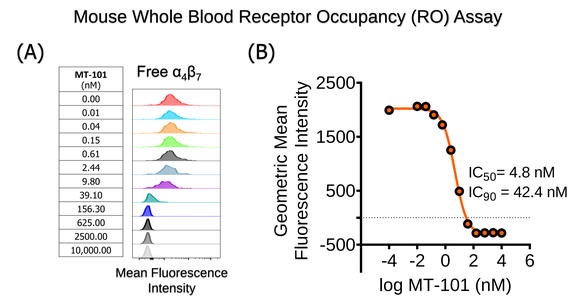

Figure 2: Inhibition of α4β7 in the mouse whole blood RO assay. *(A) Mean fluorescence intensity (MFI) histograms show reduction in free α4β7 (left) signal at low doses of MT-101. (B) Non-linear regression curve of geometric MFI showing MT-101 as a potent inhibitor of α4β7 on $CD4^+CD44^{hi}$ memory T cells in mouse whole blood RO assay.*

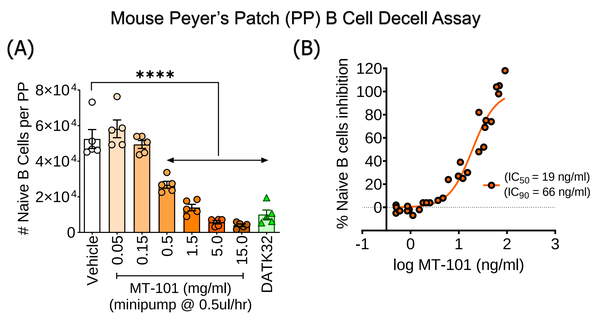

Figure 3: α4β7 inhibition potently arrests IgD+IgM+ naïve B cell trafficking to mouse Peyer's patches. *(A) MT-101 shows dose-dependent inhibition of naïve B cells per Peyer's patches (PP). DATK32, anti-mouse α4β7 blocking antibody. (B) Non-linear regression curve of % inhibition of naïve B cells in PP in response to plasma MT-101 drug exposure. Data in (B) normalized to vehicle and the highest inhibitory dose group (15 mg/ml) to set lower boundary and higher boundary, respectively. ****p <0.0001, compared to vehicle; One-way ANOVA with Dunnett's Multiple Comparisons Test.*

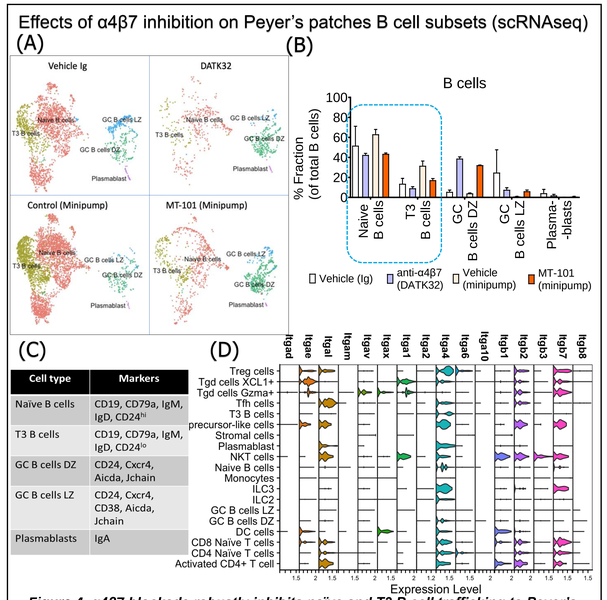

Cell type	Markers
Naive B cells	CD19, CD79a, IgM, IgD, $CD24^{hi}$
T3 B cells	CD19, CD79a, IgM, IgD, $CD24^{lo}$
GC B cells DZ	CD24, Cxcr4, Aicda, Jchain
GC B cells LZ	CD24, Cxcr4, CD38, Aicda, Jchain
Plasmablasts	IgA

Figure 4. α4β7 blockade robustly inhibits naïve and T3 B cell trafficking to Peyer's patches. *(A) UMAP plot depicting changes in B cell subsets under different treatments, (B) graphical summary of B cell fraction changes in (A), and (C) phenotypic markers for defining various B cell subsets in the PP tissue of naïve C57BL/6 mice. (D) Expression of various cell adhesion and trafficking molecules including integrins α4 and β7 in $CD45^+$ cell types in the Peyer's patches of C57BL/6 mice. The data are pooled from 3-5 mice per treatment group.*

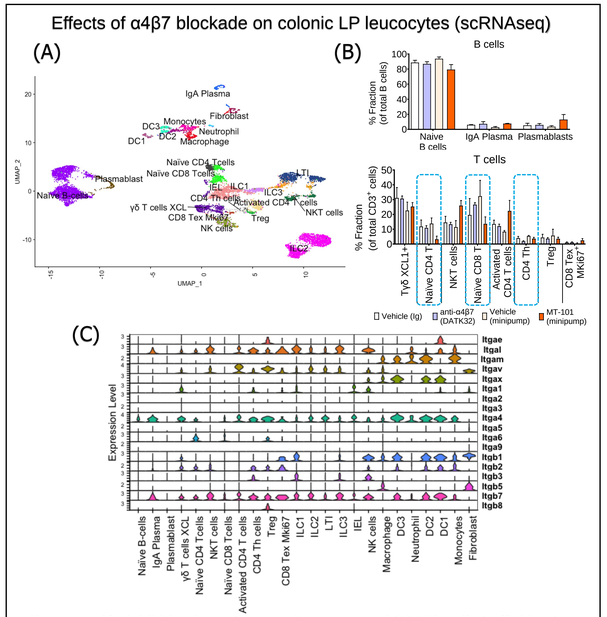

Figure 5. α4β7 inhibition impacts naïve B, naïve T, and CD4 Th cells trafficking to colonic LP. *(A) UMAP plot depicting summary of $CD45^+$ immune cell subsets detected in all colonic LP samples, (B) Graphical summary of B cells and T cell subset changes in colonic LP. (C) Violin plot showing the expression of major cell adhesion and trafficking molecules including integrins α4 and β7 in LP immune cells. The data are pooled from 3-5 mice per treatment group.*

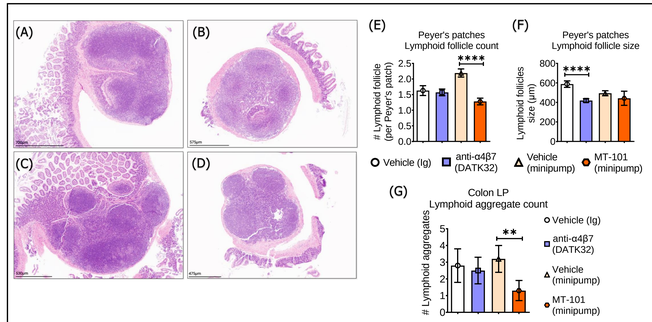

Figure 6. α4β7 inhibition diminishes secondary lymphoid structure presence in Peyer's patches and colonic lamina propria. *Histological analysis by H&E staining showing the representative size of largest lymphoid follicle as scale (in µm) from resected Peyer's patches of mice treated with (A) isotype Ig, (B) DATK32, (C) vehicle (minipump), and (D) MT-101 (minipump). Graphical summary of lymphoid follicle count and size of the largest follicle in Peyer's patches (E, F), and the mucosal lymphoid aggregate count in colonic LP (G). The data are representative (A-D) or pooled (E-G) from 6 mice per treatment group. **p <0.01, ****p <0.0001; One-way ANOVA with Tukey's Multiple Comparisons Test.*

CONCLUSIONS

- α4β7 inhibition with SMi MT-101 robustly inhibits lymphocyte trafficking to mouse GALT and colonic LP, and attenuates gut secondary lymphoid tissue architecture
- Blockade of α4β7 specifically inhibited naïve and T3 B lymphocytes trafficking to Peyer's patches, and naïve B, naïve T, and CD4 Th lymphocytes in the colonic LP.
- The pharmacological effects of α4β7 SMi on lymphocyte trafficking fully replicate that of the anti-α4β7 blocking antibody
- The profound inhibition of B cell trafficking and diminution of gut lymphoid structures upon α4β7 blockade support further investigation into the contribution of B cells to disease and response to therapy.